Geochemistry of trace elements associated with Fe and Mn nodules in the sediment of limed boreal lakes

Submission to Environmental Sciences: Processes & Impact

Authors: Raoul-Marie Couture[1,2,*], Atle Hindar[3], Sigurd Rognerud[4]

*Corresponding author: rmc@niva.no

1- Norwegian Institute for Water Research-NIVA, Gaustadalléen 21, 0349 Oslo, Norway

2- University of Waterloo, Earth and Environmental Sciences, Ecohydrology Group, 200 University Avenue West, N2L3G2, Waterloo, Canada

3- NIVA Region South, Jon Lilletuns vei 3, 4879 Grimstad, Norway.

4- NIVA Region East, Sandvikaveien 59, 2312 Ottestad, Norway.

ABSTRACT

Thousands of boreal lakes were limed for decades in Scandinavia to counteract the effect of anthropogenic acidification. We measured the concentrations of alkali earth metals (Ca, Mg, Ba), metals (Mn, Fe, Al, Co, Cd, Pb, Zn), metalloids (As, Mo) and phosphorus (P) in 165 surface sediment samples from 17 limed lakes, as well as the sediment column and porewater of two lakes chosen from this set. We report that formation of ferromanganese nodules is widespread in limed lakes, and that those nodules are enriched in trace elements, reaching for example 11500, 908 and 40 μg/g for Ba, Mo and As, respectively. Nodules are more abundant between the littoral and the profundal zones. Intense redox cycling of Fe and Mn at the sediment-water interface have redistributed trace elements in the sediment column. Ba, Co, Mo, Pb and Zn partitioned with Mn (oxy)hydroxides and As and P with Fe (oxy)hydroxides. Fe, Mo, Co and As remobilized to the porewater also diffused downward and were likely sequestrated with sulfides. We conclude that the diagenetic redistribution and partitioning of trace elements onto Fe-Mn nodules, rather than direct inputs of from liming, is the cause of the elevated trace elements burden in surface sediments.

INTRODUCTION

Acidification due to transboundary air pollution has affected lakes and rivers in vulnerable areas in Northern Europe for almost a century [1]. In the 1980s international negotiations were initiated under the auspices of the United Nations Economic Commission for Europe with the aim of reducing the emissions of acidifying air pollutants. Simultaneously, research began in Norway and Sweden on the feasibility of large-scale addition of limestone and other neutralising substances to lakes and rivers as a geoengineering measure to counteract the effect of acid deposition [2]. Such programs remain the largest lake geoengineering endeavours to date.

Owing to pollution prevention, emissions of sulfuric and nitrous gases have been reduced substantially over the last few decades [3], and the affected water bodies show clear signs of recovery [1, 4]. However, many lakes are still acidified and remediation programmes are thus still operating. Water chemical and biological effects of liming are fairly well documented from the associated research and monitoring projects [2], and the liming operations have since been optimized on the basis of these results.

Nevertheless, the target pH of 6.0-6.2 has been frequently exceeded throughout the liming period, particularly at the sediment-water interface (SWI) [5]. Overdosing of lakes for use as liming reservoirs in the watershed and incomplete dissolution of coarse liming powder during settling both lead to residual calcite persisting at the SWI[6]. Under such conditions, a local pH of 7.0-7.5, which is much higher than the typical pre-acidified reference pH of 5.5-6.0, can be reached[7]. Several studies have reported on the high trace element content in the surface sediment of such lakes [5, 8-10], coining the term "metal bomb" to express the concern that high trace element fluxes might occur upon natural re-acidification after liming [11].

Lake geoengineering techniques are under scrutiny due to the difficulty in predicting long term feedbacks in lake systems [12-14]. In this context, we document the geochemical conditions prevailing at SWI of 17 limed boreal lakes to illuminate the geochemical legacy of the liming of anthropogenically acidified boreal lakes. We report on the presence of ferromanganese (Fe-Mn) nodules, their high trace elements content, and their influence on the post-depositional mobility of a suite of major and trace elements. We interpret depth profiles of porewater concentrations of these elements to reveal diagenetic patterns and gain insights into the mechanisms responsible for trace element enrichments.

MATERIALS AND METHODS

Study sites

We refer to either regional survey lakes (17 lakes) or focus lakes (a subset of 2 lakes). The lakes were part of the national Norwegian liming program, although in some cases liming had stopped at the time of sampling. The limed lakes of the survey are located in southern Norway (Fig. 1). Coordinates and lake characteristics are given in Table SI-1 and SI-2, respectively, of the Supporting Information (SI). Lake surface area ranged from 0.06 to 6.01 km^2, catchment area from 1.2 to 128.5 km^2 and maximum depths from 11 to 118 m. Selection criteria were geographical location, size, summer thermal stratification, and the duration of liming treatment. All lakes chosen had been limed for ≥9 years. Lakes Breisjøen and Djupøyungen, hereafter referred to as Lake 1 and 8, respectively, were selected for further study at the SWI. Both lakes are in forested catchments, with the bedrock of Lake 1 being mostly granite and gneiss, and that of Lake 8 mostly porphyritic granite[1515]. The lakes differ with respect to their water residence time and liming dosage (Table 1). Due to its the short residence time, Lake 1 has been limed with a high dose relative to its area and volume. Lakes outlet pH values spanned the range of 4.88 to 6.86. Lakes 1, 3 and 17 had the low pH (4.88-5.53), consistent with reduced or terminated liming treatment, whereas Lakes 7, 8, 9 and 13 had the highest pH, > 6.7. TOC in the lakes from the regional survey ranged from 2.0 to 24.8 (Table SI-2; $\bar{x}$ = 8.9 mg/L). All lakes except Lakes 4 and 16 are thus of humic type (TOC >5 mg/L).

Sampling

~10 undisturbed sediment cores were sampled in each the 17 lakes during 2011-2012 using a modified Kajak-Brinkhurst gravity-type core (8.3 cm inner-diameter), yielding 165 intact cores.

78 Coring sites were spread evenly over the lake areas, avoiding shallow, wind-exposed parts with
79 limited sedimentations. Cores were sectioned to retrieve the upper 2 cm layer, and, in every
80 second core, an additional deep layer below 35 cm was sampled. Given the expected sediment
81 burial rates at the sites of 1-2 mm/yr, a previous study referred to the sediment below 35 cm
82 depth as a reference for pre-acidification, pre-liming conditions[16]. A grab water sample was
83 taken in an acid-washed HDPE bottles at the outlet of the survey lakes. Lakes 1 and 8 were
84 visited again on June 24th 2015 and samples were taken at three sampling sites, defined as
85 littoral, intermediate and profundal. The cores were extruded on-site, and sectioned into 1 cm
86 slices, from the SWI to 10 cm depth. The slices were placed in acid-washed polyethylene cups
87 and kept at 4 ^{o}C until freeze-drying and analysis.

88 Porewater was retrieved at a 1 cm vertical resolution from another set of three undisturbed
89 sediment cores in these two lakes, using Rhizon samplers (Rhizosphere Research Products, NL)
90 comprising of a hydrophilic porous polymer tube, with a pore diameter of 0.1 µm, extended with
91 a polyvinyl chloride tube. 4-6 ml of porewater was retrieved with vacuum-sealed vials, passing
92 through the 0.1 µM membrane, and stabilised with 2% HNO_3 upon retrieval to prevent Fe and
93 Mn precipitation.

94 Finally, the water columns were profiled from the surface down to the sediment-water interface
95 with a YSI 6600-V2 multi-parameter probe for measuring pH, temperature, and oxygen
96 saturation. Both lakes 1 and 8 had a thermocline established at 5 m at the time of sampling, with
97 oxygen saturation in the hypolimnion at 67% and 60% for Lake 1 and 8, respectively.

98 When metal nodules were observed at the sediment surface upon sampling, separate cores were
99 taken at the same site to collect a nodule subsample. Nodules were harvested by gently flushing

100 the organic material off with lake water and by further rinsing them with DI water. The nodules
101 were then placed in acid-washed polyethylene cups and stored at 4 ^{o}C until drying and analysis.

102 **Analyses**

103 Porewater, sediments and nodules were analyzed for Mn, Fe, Al, Ca, Mg, Ba, Co, Cd, P, As, Mo,
104 Pb, Zn and S concentrations by inductively coupled plasma mass-spectrometry (ICPMS Agilent
105 7700x, quadrupole with collision cell in He mode), either directly in the acidified porewater
106 sample, or after micro-wave assisted sample digestion of the sediment and nodules in
107 concentrated HNO_3. The reference material used were the TMDW (HP Standard, USA) and the
108 SLRS-6 (NRC, Canada). Precision was < 7% relative standard deviation and accuracy was
109 within 15%. Total organic carbon (TOC) was analyzed by the UV persulfate methods on a TOC-
110 TC analyzer (Phoenix 8000) and sulfate (SO_4^{2-}) by ion chromatography (Dionex ISC-2000).

111 **Thermodynamic modelling**

112 Dominant species for Ba, Co, Cd, P, As, Mo, Pb and Zn were modelled in two distinct zones of
113 the sediment column: (1) a zone at the SWI, oxygenated and rich in Fe-Mn (oxy)hydroxides and
114 (2) a zone below the depth of SO_4^{2-} removal. Saturation indices (SI = log IAP/K_{sp}, where IAP is
115 the ion activity product and K_{sp} the solubility product) of the aqueous phase with respect to
116 various mineral phase were calculated in both zones using the public domain computer code
117 PHREEQC version v.3.1.2 [17]. Cation binding to dissolved organic matter (DOM) and adsorption
118 of trace elements onto both Fe and Mn (oxy)hydroxides was calculated only in the first zone
119 using the software Visual MINTEQ 3.1 (http://vminteq.lwr.kth.se). The NICA-Donnan [18] model
120 was used for cation binding to DOM and configured using measured DOC, pH and aqueous
121 concentrations. The concentrations of humic acids (HA) and fulvic acids (FA) were estimated

from DOC concentrations assuming that DOM contains 50% C and a FA:HA ratio of 9:1[19]. Two surface complexation models (SCM) were configured to calculate adsorption: (1) trace element adsorption onto Fe (oxy)hydroxides and cation adsorption onto Mn (oxy)hydroxides relied on the Double Layer model (DLM)[20, 21], and (2) P, As and Mo adsorption onto Mn (oxy)hydroxides relied on the Triple Layer model (TLM)[22, 23]. The use of the TLM was necessary because, to our knowledge, there is no set of constants for the adsorption of P, As and Mo onto Mn (oxy)hydroxides that builds on the DLM model. Equilibrium calculations were performed fixing a temperature of 10 °C, the total concentration of aqueous constituents, and the amount of solid-phase Fe and Mn in excess at the SWI[24] to determine the amount of element bound to DOM or adsorbed to metal surfaces that is consistent with the total measured aqueous concentrations. Thermodynamic constant added to the MINTEQ databases used with Visual MINTEQ and PHREEQC are listed in Table SI-3.

RESULTS AND DISCUSSIONS

Influence of liming on the formation of Fe-Mn nodules

The average concentrations of Mn were 6-fold higher at the surface ($\bar{x}$ = 31 mg/g) than at the reference depth ($\bar{x}$ = 4.8 mg/g) in the sediment of the survey lakes (*n*=165). Fe was also higher at the surface by a factor 1.3. The highest concentration of Fe (201 mg/g) and Mn (81 mg/g) were measured in the two focus Lakes 1 and 8, respectively (Fig. 2a). Binning the number of cores with Mn enrichments factors >4 (*n*=57) in the littoral, intermediate or profundal categories reveal that enrichments are more frequent at water-column depths between the littoral and the profundal zones (Fig. 2b). This distribution suggests an in-lake process whereby oxygen depletion — sporadic during late summer and likely enduring under ice [25] — forces dissolved Mn out of the

144 sediment to the overlying water, then towards oxic conditions where Mn accumulates as
145 (oxy)hydroxides at the SWI [26, 27].

146 Porewater Mn profiles exhibit features consistent with Mn recycling [24, 26]. Solid-phase Mn
147 decreases sharply just below the SWI, concurrent with an increase in porewater Mn (Fig. 3a and
148 k). Porewater Fe concentration profiles also display evidence of the reductive dissolution of
149 (oxy)hydroxides below 2-3 cm depth, and of the precipitation of Fe below the SWI. The
150 porewater Fe concentrations are twice as high in Lake 1 than in Lake 8, reaching 12 mg/L and 4
151 mg/L, respectively (Fig. 3d-f, m-o).

152 Black-brown nodules of sizes 0.05-3 cm were found in the surficial sediment of 7 of the survey
153 lakes, including Lakes 1 and 8 (Fig. SI-3) with average Mn and Fe concentrations of 324 and 326
154 mg/g, respectively (Table 2). Nodule sizes are consistent with the hypothesis that liming
155 triggered their formation. Using 10 to 20 years as the typical period of elevated pH during and
156 after liming, and an average nodule radius of 10 mm, we estimate a growth rate of 0.5 to 1
157 mm/yr at our sites, also consistent with previous growth rate estimates for lakes in the northeast
158 United-States [28] or at the sediment-seawater interface [,29]. Although metal nodules are frequently
159 reported in lakes[27, 28, 30-33], we are not aware of such reports for acidic or formerly acidic humic
160 lakes. Surveys of >1500 non-limed Norwegian lakes [16] and of limed lakes from Sweden [10] did
161 not report on nodules.

162 Fe-rich accretions formed via the rapid oxidation of Fe(II) by $O_{2(aq)}$ have been observed in
163 several lakes and bogs [34], and at times harvested as Fe ore [35]. Mn enrichments are less frequent
164 because Mn(II) oxidation requires a pH typically > 7.5 to proceed [36] and is the kinetically
165 limiting factor in nodule formation[29]. Here, Mn (oxy)hydroxides precipitation was likely

166 unfavorable until $CaCO_3$ particles reaching the SWI increased the pH and favored nucleation of
167 the Fe-Mn precipitate[37].

168 Results on Ca and Mg suggest that liming residuals persist at or below the SWI, influencing local
169 pH. The concentrations of Ca and Mg, major constituents of the liming powders, were generally
170 higher by a factor ~2 in the surface sediments than at depth. Sub-surface peaks of Ca are buried
171 at 2 cm depth in Lake 1, consistent with liming operations ending 13 years ago. In contrast, Ca is
172 enriched at the SWI in Lake 8. In Lake 1, a pH of 5.0 in the epilimnion, decreasing to 4.45 in the
173 hypolimnion, suggest that the lake is returning to pre-liming pH values, likely influenced by high
174 organic acids concentrations and a short water residence time. In contrast, in Lake 8, the pH of
175 Lake 8 was 6.3 in the epilimnion, decreasing to 5.3 in the hypolimnion. The higher pH in Lake 8
176 is consistent with the more recent termination of the liming treatment in 2013, the longer water
177 residence time. The high Mg:Ca ratio in the surface sediment (0.11-0.75) relative to the ratio in
178 the calcite powder materials (0.005-0.056) suggest an enrichment in Mg-containing carbonate
179 minerals such as dolomite [38] , which can sustain elevated pH and thus Mn (oxy)hydroxides
180 precipitation.

181 **Diagenetic redistribution of trace elements at the sediment-water interface**

182 Fe-Mn nodules are known to scavenge elements from lake water [28, 31, 39, 40] via co-precipitation,
183 as their growth provides renewed surfaces for element sorption [41]. Measurements of the trace
184 element content of the nodules from the lake survey reveals high concentrations of Ba, Zn and
185 Mo, reaching 11500, 3250 and 908 μg/g, respectively (Table 2), at the high-end of the ranges
186 provided in Table 2 for published trace-element concentrations measured in nodules from other
187 lakes. These enrichments lead to bulk concentrations several fold higher than those reported in
188 the literature for representative lake sediments [10, 42-44]. The case of Mo is particularly singular:

189 solid-phase Mo in Lake 8 is >3 orders of magnitude higher than what was previously reported for
190 boreal lakes under the influence of a metal smelter [44], while in Lake 1 Mo values are close to the
191 reported average for surface lake sediments [16].

192 Such trace element burden in the sediments cannot be explained by direct input from liming
193 powder (See Text SI-1 and Table SI-5). Instead, scavenging of trace elements driven by Fe and
194 Mn diagenesis at the SWI stands as the main driver behind the elevated trace elements
195 concentrations measured here. Results from surface complexation modelling, summarized in
196 Table SI-4, suggest that Ba (with adsorption complex ≡MnO-Ba^{+}), Co (≡Mn-Co^{+}), Mo (≡MnO-
197 $HMoO_4$) as well as Pb (≡MnO-Pb^{+}) and Zn (≡MnO-Zn^{+}) are overall predominantly sorbed onto
198 to Mn (oxy)hydroxides. Consistent with those predictions, solid-phase Ba is enriched below the
199 SWI (Fig. 4a and k) in the same cores than those with strong Mn enrichments (Fig. 3a and k), as
200 frequently reported in the literature on Fe-Mn nodules[30, 31]. Co, at the SWI in Lake 1 (Fig. 4d-f),
201 and Mo, at the intermediate site of Lake 8 (Fig. 5q), are also enriched. Porewater peaks of Ba, Co
202 and Mo are found along with those of Mn below the SWI, which suggests remobilisation
203 following the reduction of Mn (oxy)hydroxides, and re-adsorption of upward diffusing elements
204 onto Mn (oxy)hydroxides at the SWI.

205 Cd is bound to Mn (≡MnO-Cd+) only at the intermediate site of Lake 8 (12 m depth). At the
206 other sites, thermodynamic modelling suggests that Cd is instead bound to DOM. The similarity
207 of solid-phase Cd profiles with those of Pb (See Fig. SI-2d-f, j-l) — a metal shown to be poorly
208 mobile post-deposition[19] — suggests that the depth profiles of both elements are little affected by
209 diagenesis as they are strongly bound to organic matter.

210 The oxyanions P (≡Fe-H_2PO_4 in Lake 1 and ≡Fe-PO_4^{2-} in Lake 8), As (≡Fe-$HAsO_4^{-}$ in Lake 1
211 and ≡Fe-AsO_4^{2-} in Lake 8) are largely sorbed onto Fe (oxy)hydroxides at all sites. Sediment P

concentrations increase from the SWI to 6 cm depth at all sites (Fig. 5a-c, j-l), reaching 3000 µg/g in Lake 1. Porewater P, which is up to 6-fold higher in Lake 1 than in Lake 8, increases from the SWI downwards in all cores, with the highest concentrations found at the deepest sites. Solid-phase As displays sub-surface peaks of 20-30 µg/g at 3-5 cm depth at all sites, but the intermediate site at Lake 1, where it shows a constant decrease from the SWI downwards. Features of the porewater As concentration profiles, similar across sites with subsurface maxima of 0.7 µg/L at 2-7 cm depth (Fig. 5d-f, m-o), point to As being released during reductive dissolution of Fe (oxy)hydroxides [45] and recycled close to the SWI, consistent with the results of the SCMs.

Sequestration mechanisms at depth

In the sediment column, porewater Fe and Mn production (Fig. 3a-c, j-l) indicate that anoxic conditions prevail below the SWI. Further, at 2-4 cm below the SWI, decrease in porewater S, from the highest values in the overlying waters (0.5 mg/L in Lake 1 and 0.8 mg/L in Lake 8; Fig. SI-1a-c, j-l), to lower values (< 0.2 mg/L), are consistent with bacterial SO_4^{2-} reduction is occurring.

At depth in the sediment column, solid-phase Fe displays a second, deeper sub-surface peak (Fig. 3. d-f, m-o). This is likely due to the formation of Fe sulfides such as amorphous mackinawite ($FeS_{m(s)}$) [46] below the depth of SO_4^{2-} reduction. SO_4^{2-} reduction is evidenced by porewater S removal, which is observed between 2-4 cm depth at all sites (Fig. SI-1a-c, j-l). The porewater sample preservation techniques by acidification will have released volatile hydrogen sulphides, such that the measured porewater S likely represents oxidized S species dominated by SO_4^{2-}. In the absence of sulfides (HS^-) measurements, we assume that porewater HS^- produced via SO_4^{2-} reduction is at equilibrium with $FeS_{m(s)}$ [47]. Given that reducing all SO_4^{2-} would yields 0.5 mg/L of

HS^-, to which porewater Fe is available in large excess, titration of HS^- by Fe is likely. In contract to Fe, solid-phase Mn concentration profiles do not exhibit sub-surface peaks, possibly due to the slow precipitation kinetics of MnS(s) [48] Rather, as summarized in Morse (1999), the main sink for reduced porewater Mn is likely rhodochrosite or dolomite analogs.

While acknowledging that such estimation of sulfide concentrations is uncertain, it allows proposing sequestration mechanisms for sulfide-bound elements that are consistent with our observations. Co enrichments between 2-6 cm depth at the intermediate and deep sites of Lake 8 (Fig 4n-o) suggest association with Fe sulfides at depth[49], in line with values of SI with respect to $CoS_{\beta(s)}$ reaching <0.5 at the deepest site. Sub-surface solid-phase Cd and Pb peaks are also seen in all cores (Fig. 4g-i, p-r and Fig. SI-2d-f, j-l, respectively), below the depth of Fe-Mn (oxy)hydroxide reduction. Sulfides are likely sinks for Cd as well as Pb, as porewater reach saturation with respect to both $CdS_{(s)}$ (Lake 8; Fig. SI-4) and $PbS_{(s)}$ (Lake 1 and 8; Fig SI-4) minerals.

Clear associations between Fe and As (Fig. 3m-o and Fig. 5m-o) as well as solid-phase Mo enrichments (Fig. 5g-i,p-r) below the depth of SO_4^{2-} reduction points to sulfides as a sink for those metalloids. Thermodynamic modelling indicates that thiolated Mo and As species are do not dominate Mo and As speciation in porewater. Further, precipitation of discrete As and Mo phases is unlikely, as the SI of realgar and orpiment is consistently <0 (Fig. SI-$) and that of $MoS_{2(s)}$ largely >0. Therefore, co-precipitation and sorption of As [24, 50, 51] and Mo [52] onto $FeS_{m(s)}$ or other Fe phases stands as a likely sequestration mechanisms.

In contrast to the oxyanions As and Mo, P does not show evidence being remobilised with Fe or of sequestration at depth. Porewater is close to saturation with respect to $MnHPO_{4(s)}$ below 2 cm depth at all sites (SI ± 0.1; Fig. SI-4), pointing to a possible control of Mn on P mobility, as was

hypothesized in estuarine sediment[53]. Alternatively, P remobilised during Fe (oxy)hydroxides dissolution can immediately re-adsorb onto a non-redox active phase such as Al oxides[54]. Al concentrations profiles (Fig. SI-1d-f, m-o) show a steady increase with depth, similar to that of P. Al:P molar ratios vary between 7 and 14 in Lake 1 and between 24 and 41 in Lake 8 (Fig. 5a-c, j-l), with the highest values found in the upper 4 cm of the sediment cores. Values of Al:P ratios >25 at Lake 8 suggest a high P-binding potential by Al[55]. Conversely, ratios <14 at Lake 1, along high porewater P concentrations, suggest a lower P-binding capacity by Al at this site. Artificial oligotrophication of limed lakes has been hypothesized to proceed via P sorption onto Al or via P association with Fe or Mn[13, 55, 56]; our data is consistent with the former hypothesis in Lake 1 and the latter in Lake 8.

Relevance in the context of recovery from acidification and current environmental changes.

Although a first approximation of the dominant trace element species formed in the presence of Fe-Mn nodule induced by lake liming, our results clearly suggest that Ba, Co , Mo, Pb and Zn partitioned with Mn (oxy)hydroxides and As and P with Fe (oxy)hydroxides at the SWI. This illustrate that the new pH regimes brought about by liming reconfigured the depth distribution of trace elements at the SWI. At depth in the sediment column, P is bound to Fe-Mn and Al oxides. The mechanisms controlling porewater Mo, Co and As concentrations at depth were not identified with certainty but likely include (co-)precipitation with sulfides. In contrast, depth profiles of Cd and Pb appeared less affected by nodule formation.

Slow dissolution of lime residuals[6] and of the Fe-Mn nodules themselves contribute to upholding pH and redox conditions after liming, mitigating the risk of a sudden pulse of trace-element. Nevertheless, a decline in pH is expected in the future and may trigger both Mn (oxy)hydroxides dissolution and the desorption of sorbed oxy-anions. Moreover, DOC is increasing in boreal

lakes[57]. DOC is a major ligand for metal(loid)s in boreal lakes[58], and can further compete with trace elements for sorption sites on (oxy)hydroxides surfaces[59, 60]. DOC is also thought to enhance anoxia[25], which will destabilise (oxy)hydroxide phases. The long term and unanticipated consequences of lake manipulation on sediment diagenesis should thus be taken into account when planning further catchment and lake manipulations in response to today's water quality issues related to anoxia[61] and harmful algae blooms [12].

Conflict of interest

There are no conflicts to declare.

Acknowledgments

We thank T.E. Eriksen, S.N. Holen, J. Håvardstun and L. Tveiten for help with field work, I. Dahl for analyses, L.B. Skancke for data handling, E. Lund for Fig. 1, A. Chappaz (Central Michigan University) and R.F. Wright (NIVA) for discussions and C. Wilson for editing the manuscript. AH and SR acknowledge funding from the Norwegian Environment Agency for the SedMetall project and RMC from the Research Council of Norway project "Lakes in Transition" (244558).

Supporting Information. Characteristics of the survey lakes, trace element content of limestone, results of flux and of thermodynamic calculations, additional thermodynamic constants, concentrations of S, Al, Mg, Pb and Zn, and pictures of nodules in Lakes 1 and 8.

Litterature cited

1. B. L. Skjelkvåle, C. Evans, T. Larssen, A. Hindar and G. G. Raddum, Recovery from Acidification in European Surface Waters: A View to the Future, *AMBIO*, 2003, **32**, 170-175.
2. T. Clair and A. Hindar, Liming for the mitigation of acid rain effects in freshwaters: A review of recent results, *Environ. Rev.*, 2005, **13**, 91-128.
3. UNECE, *The 1999 Gothenburg Protocol to Abate Acidification, Eutrophication and Ground-level Ozone.* , UNECE Convention on Long-range Transboundary Air Pollution. , 1999.
4. J. Caputo, C. M. Beier, H. Fakhraei and C. T. Driscoll, Impacts of Acidification and Potential Recovery on the Expected Value of Recreational Fisheries in Adirondack Lakes (USA), *Environ. Sci. Technol.*, 2017, **51**, 742-750.
5. T. Wällstedt, Lime Residues and Metal Sequestration in Sediments of Excessively Limed Lakes, *Water Air Soil Poll.*, 2011, **219**, 535-546.
6. A. Hindar and R. F. Wright, Long-term records and modelling of acidification, recovery, and liming at Lake Hovvatn, Norway, *Can. J. Fish. Aquat. Sci.*, 2005, **62**, 2620-2631.
7. R. F. Wright, T. Larssen, L. Camarero, B. J. Cosby, R. C. Ferrier, R. Helliwell, M. Forsius, A. Jenkins, J. Kopacek, V. Majer, F. Moldan, M. Posch, M. Rogora and W. Schopp, Recovery of acidified European surface waters, *Environ. Sci. Technol.*, 2005, **39**, 64A-72A.
8. D. O. Andersen and J. Pempkowiak, Sediment content of metals before and after lake water liming, *Sci. Total Environ.*, 1999, **243**, 107-118.
9. T. Wällstedt and H. Borg, Metal burdens in surface sediments of limed and nonlimed lakes, *Sci. Total Environ.*, 2005, **336**, 135-154.
10. T. Wällstedt, H. Borg, M. Meili and C. M. Morth, Influence of liming on metal sequestration in lake sediments over recent decades, *Sci. Total Environ.*, 2008, **407**, 405-417.
11. E. Lydersen and S. Löfgren, Potential Effects of Metals in Reacidified Limed Water Bodies in Norway and Sweden, *Environ. Monit. Access.*, 2002, **73**, 155-178.
12. M. Lürling, E. Mackay, K. Reitzel and B. M. Spears, Editorial – a critical perspective on geo-engineering for eutrophication management in lakes, *Water Res.*, 2015, **97**, 1-10.
13. Q. Hu and B. J. Huser, Anthropogenic oligotrophication via liming: Long-term phosphorus trends in acidified, limed, and neutral reference lakes in Sweden, *AMBIO*, 2014, **43**, 104-112.
14. B. M. Spears, S. C. Maberly, G. Pan, E. Mackay, A. Bruere, N. Corker, G. Douglas, S. Egemose, D. Hamilton, T. Hatton-Ellis, B. Huser, W. Li, S. Meis, B. Moss, M. Lürling, G. Phillips, S. Yasseri and K. Reitzel, Geo-Engineering in Lakes: A Crisis of Confidence?, *Environ. Sci. Technol.*, 2014, **48**, 9977-9979.
15. National bedrock database http://geo.ngu.no/kart/berggrunn/?lang=English, (accessed 01/03/2017, 01/03/2017).
16. S. Rognerud and E. Fjeld, Trace Element Contamination of Norwegian Lake Sediments, *AMBIO*, 2001, **30**, 11-19.
17. D. L. Parkhurst and C. A. J. Appelo, in *U.S. Geological Survey Techniques and Methods*, available only at http://pubs.usgs.gov/tm/06/a43/. 2013, ch. A43, pp. 1-497.

18. D. G. Kinniburgh, C. J. Milne, M. F. Benedetti, J. P. Pinheiro, J. Filius, L. K. Koopal and W. H. VanRiemsdijk, Metal ion binding by humic acid: Application of the NICA-Donnan model, *Environ. Sci. Technol.*, 1996, **30**, 1687-1698.
19. C. Gallon, A. Tessier, C. Gobeil and M. C. Alfaro-De la Torre, Modeling diagenesis of lead in sediments of a Canadian Shield lake, *Geochim. Cosmochim. Acta*, 2004, **68**, 3531-3545.
20. D. A. Dzombak and F. M. M. Morel, *Surface Complexation Modeling: Hydrous Ferric Oxide*, Wiley, New York, 1990.
21. J. W. Tonkin, L. S. Balistrieri and J. W. Murray, Modeling Sorption of Divalent Metal Cations on Hydrous Manganese Oxide Using the Diffuse Double Layer Model, *Appl. Geochem.*, 2004, **19**, 29-53.
22. S. C. Ying, B. D. Kocar and S. Fendorf, Oxidation and competitive retention of arsenic between iron- and manganese oxides, *Geochim. Cosmochim. Acta*, 2012, **96**, 294-303.
23. L. S. Balistrieri and T. T. Chao, Adsorption of Selenium by Amorphous Iron Oxyhydroxide and Manganese-Dioxide, *Geochim. Cosmochim. Acta*, 1990, **54**, 739-751.
24. R.-M. Couture, C. Gobeil and A. Tessier, Arsenic, iron and sulfur co-diagenesis in lake sediments, *Geochim. Cosmochim. Acta*, 2010, **74**, 1238–1255.
25. R.-M. Couture, H. A. De Wit, K. Tominaga, P. Kiuru and I. Markelov, Oxygen dynamics in a boreal lake responds to long-term changes in climate, ice phenology, and DOC inputs, *J. Geophys. Res.: Biogeosciences*, 2015, **120**, 2441–2456.
26. R. W. Macdonald and C. Gobeil, Manganese Sources and Sinks in the Arctic Ocean with Reference to Periodic Enrichments in Basin Sediments, *Aquat. Geochem.*, 2012, **18**, 565-591.
27. V. A. Dauval'ter and B. P. Il'yashuk, Conditions of formation of ferromanganese nodules in the bottom sediments of lakes in the Baltic shield, *Geochem. Int.* , 2007, **45**, 615-619.
28. C. A. Asikainen and S. F. Werle, Accretion of ferromanganese nodules that form pavement in Second Connecticut Lake, New Hampshire, *PNAS*, 2007, **104**, 17579-17581.
29. B. P. Boudreau, Metals and models: Diagenetic modelling in freshwater lacustrine sediments, *J. Paleolimnol.*, 1999, **22**, 227-251.
30. Y. N. Vodyanitskii, Mineralogy and geochemistry of manganese: A review of publications, *Eurasian Soil Sci.* , 2009, **42**, 1170-1178.
31. W. S. Fyfe, B. I. Kronberg, M. Peirce and G. G. Leppard, Ferromanganese Nodules from Lake Ontario (Bay of Quinte): Minor Element Geochemistry, *J. Great Lakes Res.*, 1980, **6**, 203-209.
32. D. N. Edgington and E. Callender, Minor element geochemistry of Lake Michigan ferromanganese nodules, *Earth. Planet. Sci. Letters*, 1970, **8**, 97-100.
33. V. N. Kuleshov and L. Y. Shterenberg, Isotopic composition of ferromanganese concretions from Lake Krasnoye, *Int. Geol. Rev.*, 1988, **30**, 1092-1103.
34. K. J. Aanes, M. Bergan and E. Iversen, *Orienterende undersøkelser i forbindelse med mulig ny gruvedrift og oppredning i Kvalsund kommune*, Norwegian Institute for Water Research-NIVA, Oslo, 2011.
35. V. Buchwald, in *Prehistoric and Medieval Direct Iron Smelting in Scandinavia and Europe: Aspects of Technology and Society*, ed. L. Norbach, Aarhus University Press, Aarhus, 2003, pp. 171-176.
36. J. J. Morgan, Kinetics of reaction between O2 and Mn(II) species in aqueous solutions, *Geochim. Cosmochim. Acta*, 2005, **69**, 35-48.

37. J. E. Post, Manganese oxide minerals: Crystal structures and economic and environmental significance, *PNAS*, 1999, **96**, 3447-3454.
38. H. U. Sverdrup, in *Acidic Precipitation: Proceedings of the International Symposium on Acidic Precipitation Muskoka, Ontario, September 15–20, 1985*, ed. H. C. Martin, Springer Netherlands, Dordrecht, 1987, DOI: 10.1007/978-94-009-3385-9_182, pp. 1881-1891.
39. Y.-T. Meng, Y.-M. Zheng, L.-M. Zhang and J.-Z. He, Biogenic Mn oxides for effective adsorption of Cd from aquatic environment, *Environ. Pollut.*, 2009, **157**, 2577-2583.
40. J. R. Bargar, C. C. Fuller, M. A. Marcus, A. J. Brearley, M. Perez De la Rosa, S. M. Webb and W. A. Caldwell, Structural characterization of terrestrial microbial Mn oxides from Pinal Creek, AZ, *Geochim. Cosmochim. Acta*, 2009, **73**, 889-910.
41. M. Kersten and D. A. Kulik, Competitive Scavenging of Trace Metals by HFO and HMO During Redox-Driven Early Diagenesis of Ferromanganese Nodules - Dedicated to Prof. Dr. Ulrich Forstner on His 65th Birthday, *J. Soil Sediments*, 2005, **5**, 37-47.
42. S. Rigaud, O. Radakovitch, R.-M. Couture, B. Deflandre, D. Cossa, C. Garnier and J.-M. Garnier, Mobility and fluxes of trace elements and nutrients at the sediment–water interface of a lagoon under contrasting water column oxygenation conditions, *Appl. Geochem.*, 2013, **31**, 35-51.
43. M. C. Alfaro-De la Torre and A. Tessier, Cadmium deposition and mobility in the sediments of an acidic oligotrophic lake, *Geochim. Cosmochim. Acta*, 2002, **66**, 3549-3562.
44. A. Chappaz, C. Gobeil and A. Tessier, Geochemical and anthropogenic enrichments of Mo in sediments from perennially oxic and seasonally anoxic lakes in Eastern Canada, *Geochim. Cosmochim. Acta*, 2008, **72**, 170-184.
45. R.-M. Couture, B. Shafei, P. Van Cappellen, A. Tessier and C. Gobeil, Non-Steady State Modeling of Arsenic Diagenesis in Lake Sediments, *Environ. Sci. Technol.*, 2010, **44**, 197–203.
46. W. Davison, The solubility of iron sulphides in synthetic and natural waters at ambient temperature, *Aquat. Sci.*, 1991, **53**, 1015-1621.
47. A. Hartland, M. S. Andersen and D. P. Hamilton, Phosphorus and arsenic distributions in a seasonally stratified, iron- and manganese-rich lake: microbiological and geochemical controls, *Environ. Chem.*, 2015, **12**, 708-722.
48. J. W. Morse and G. W. Luther, Chemical influences on trace metal-sulfide interactions in anoxic sediments, *Geochim. Cosmochim. Acta*, 1999, **63**, 3373-3378.
49. J. Hamilton-Taylor, W. Davison and K. Morfett, The biogeochemical cycling of Zn, Cu, Fe, Mn, and dissolved organic C in a seasonally anoxic lake, *Limnol. Oceanogr.*, 1996, **41**, 408-418.
50. E. D. Burton, S. G. Johnston and B. D. Kocar, Arsenic mobility during flooding of contaminated soil: the effect of microbial sulfate reduction, *Environ. Sci. Technol.*, 2014, DOI: 10.1021/es503963k.
51. R.-M. Couture, J. C. Rose, N. Kumar, K. Mitchell, D. Wallschläger and P. Van Cappellen, Sorption of arsenite, arsenate and thioarsenates to iron oxides and iron sulfides: a kinetic and spectroscopic investigation, *Environ. Sci. Technol.*, 2013, **47**, 5652–5659.

52. T. W. Dahl, A. Chappaz, J. P. Fitts and T. W. Lyons, Molybdenum reduction in a sulfidic lake: Evidence from X-ray absorption fine-structure spectroscopy and implications for the Mo paleoproxy, *Geochim. Cosmochim. Acta.*, 2013, **103**, 213-231.
53. S. Carroll, P. A. O'Day, B. Esser and S. Randall, Speciation and fate of trace metals in estuarine sediments under reduced and oxidized conditions, Seaplane Lagoon, Alameda Naval Air Station (USA), *Geochem. Trans.*, 2002, **3**, 81.
54. J. Kopáček, J. Hejzlar, J. Kaňa, S. A. Norton and E. Stuchlík, Effects of Acidic Deposition on in-Lake Phosphorus Availability: A Lesson from Lakes Recovering from Acidification, *Environ. Sci. Technol.*, 2015, **49**, 2895-2903.
55. J. Kopáček, J. Borovec, J. Hejzlar, K.-U. Ulrich, S. A. Norton and A. Amirbahman, Aluminum Control of Phosphorus Sorption by Lake Sediments, *Environ. Sci. Technol.*, 2005, **39**, 8784-8789.
56. T. Wilson, A. Amirbahman, S. Norton and M. Voytek, A record of phosphorus dynamics in oligotrophic lake sediment, *J. Paleolimnol.*, 2010, **44**, 279-294.
57. D. T. Monteith, J. L. Stoddard, C. D. Evans, H. A. De Wit, M. Forsius, T. Hogasen, A. Wilander, B. L. Skjelkvale, D. S. Jeffries, J. Vuorenmaa, B. Keller, J. Kopacek and J. Vesely, Dissolved organic carbon trends resulting from changes in atmospheric deposition chemistry, *Nature*, 2007, **450**, 537-539.
58. O. S. Pokrovsky, L. S. Shirokova, S. A. Zabelina, T. Y. Vorobieva, O. Y. Moreva, S. I. Klimov, A. V. Chupakov, N. V. Shorina, N. M. Kokryatskaya, S. Audry, J. Viers, C. Zoutien and R. Freydier, Size Fractionation of Trace Elements in a Seasonally Stratified Boreal Lake: Control of Organic Matter and Iron Colloids, *Aquatic Geochemistry*, 2012, **18**, 115-139.
59. J. P. Gustafsson, Modelling molybdate and tungstate adsorption to ferrihydrite, *Chem. Geol.*, 2003, **200**, 105-115.
60. W. H. van Riemsdijk, L. K. Koopal, D. G. Kinniburgh, M. F. Benedetti and L. Weng, Modeling the Interactions between Humics, Ions, and Mineral Surfaces, *Environ. Sci. Technol.*, 2006, **40**, 7473-7480.
61. R. Gachter and B. Wehrli, Ten years of artificial mixing and oxygenation: No effect on the internal phosphorus loading of two eutrophic lakes, *Environ. Sci. Technol.*, 1998, **32**, 3659-3665.
62. K. H. Wedepohl, The Composition of the Continental-Crust, *Geochim. Cosmochim. Acta*, 1995, **59**, 1217-1232.

469 **Table 1**. General characteristics, liming regime, and water chemistry for the two focus lakes.

	Lake 1	**Lake 8**
Lake characteristics		
Name	Breisjøen	Djupøyungen
Area (km^2)	0.59	0.21
Maximum depth (m)	20	20
Volume ($\times 10^6$ m^3)	2.20	1.55
Catchment area (km^2)	27.2	1.2
Water residence time (yr)	0.2	2.0
Liming regime		
Liming period	1993-2001	1995-2011
Average dose (tons)	53	6
Areal dose (t/km^2)	90	29
Volumetric dose (g/m^3)	24.1	3.9
Water chemistry		
pH[a]	4.4-5.0	5.3-6.3
TOC (mg/L) [b]	13	5.3
Ca (mg/L) [b]	1.1	4.8
SO_4^{2-} (mg/L) [b]	1.1	2.0

a:Water column range.
b:At lake outlet.

470

471 **Table 2.** Range of concentrations for selected elements in the nodule found at the surface of 7 of
472 the 17 survey lakes. Values in mg/kg dry weight.

	This study			Literature values	
Element	**Mean**	**Min**	**Max**	**Fe-Mn nodules[28, 31]**	**Earth Crust[62]**
Mn	170100	90800	326000	2000-320000	7160
Fe	214775	16400	324000	90000-320000	43200
Ca	4134	2560	6630	1000-5000	38500
Mg	829	165	2240	100-1000	22000
Ba	4366	422	11500	79-4748	584
Co	54.1	20.6	90.6	59-305	24
Cd	2.50	0.35	9.53	1-12	0.1
P	478	200	621	1000-2000	757
As	16.8	0.3	39.8	10-475	1.7
Mo	239	3.30	908	1-16	1.1
Pb	72.3	3	139	3-130	13
Zn	682	79	3250	309-774	65

473

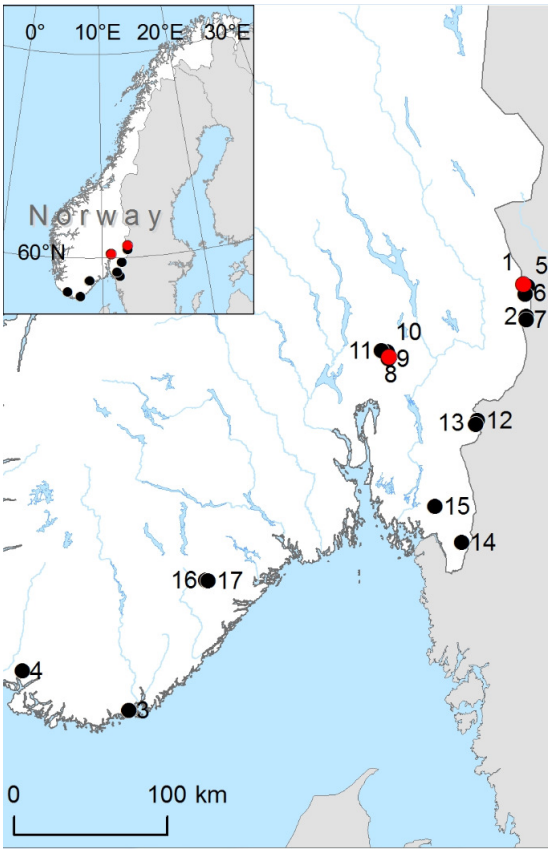

Figure 1. Location of regional survey lakes (black) and of the two focus lakes (red).

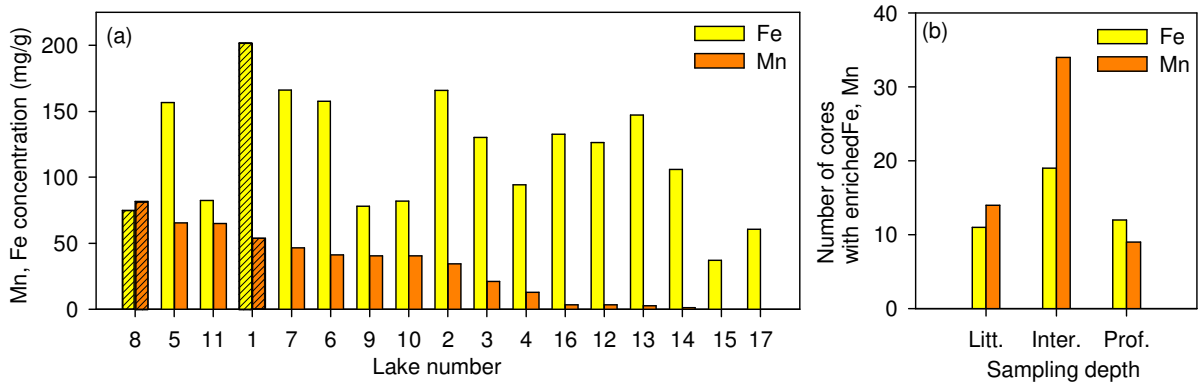

478

479 **Figure 2.** Panel (a) Concentrations of Fe and Mn in the uppermost 2 cm of the regional survey
480 lakes, ranked by order of decreasing Mn concentrations. The focus Lakes 8 and 1 are identified
481 by diagonal stripes. Panel (b) Number of cores, from the 17 lakes survey, with Mn enrichment >
482 4 or Fe enrichment >2, found at littoral, intermediate and profundal sites. These three categories
483 are defined as vertical sampling depth to max depth ratios >0.3 (littoral), between 0.3 and 0.6
484 (intermediate), and >0.6 (profundal), respectively.

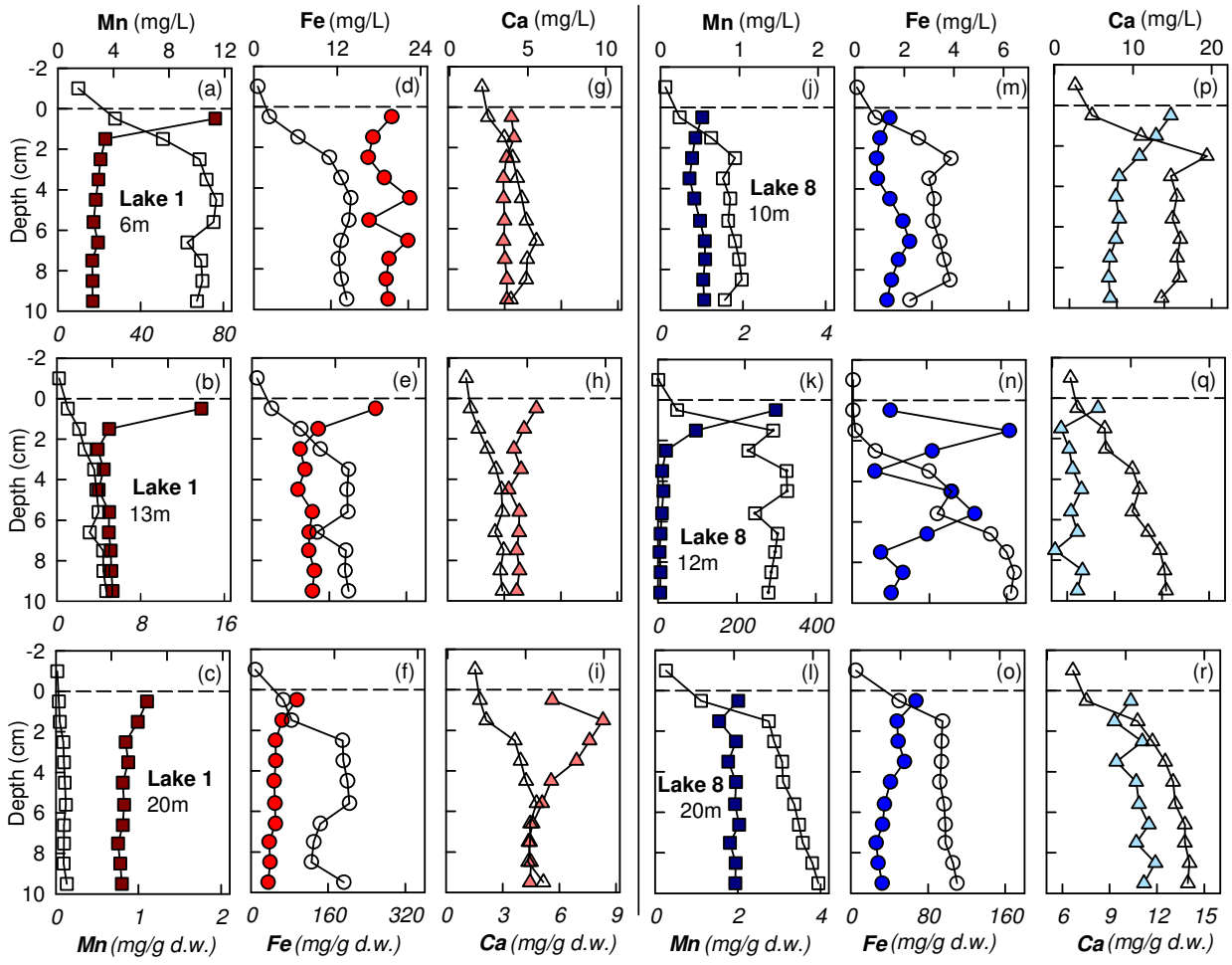

485

486 **Figure 3.** Depth profiles of sedimentary (closed symbol) and porewater (open symbol) Mn (a-c,

487 j-l), Fe (d-f, m-o), and Ca (g-i, p-r) in Lake 1 (left panels a-i) and Lake 8 (right panels j-r).

488 Horizontal dashed lines indicate the sediment-water interface.

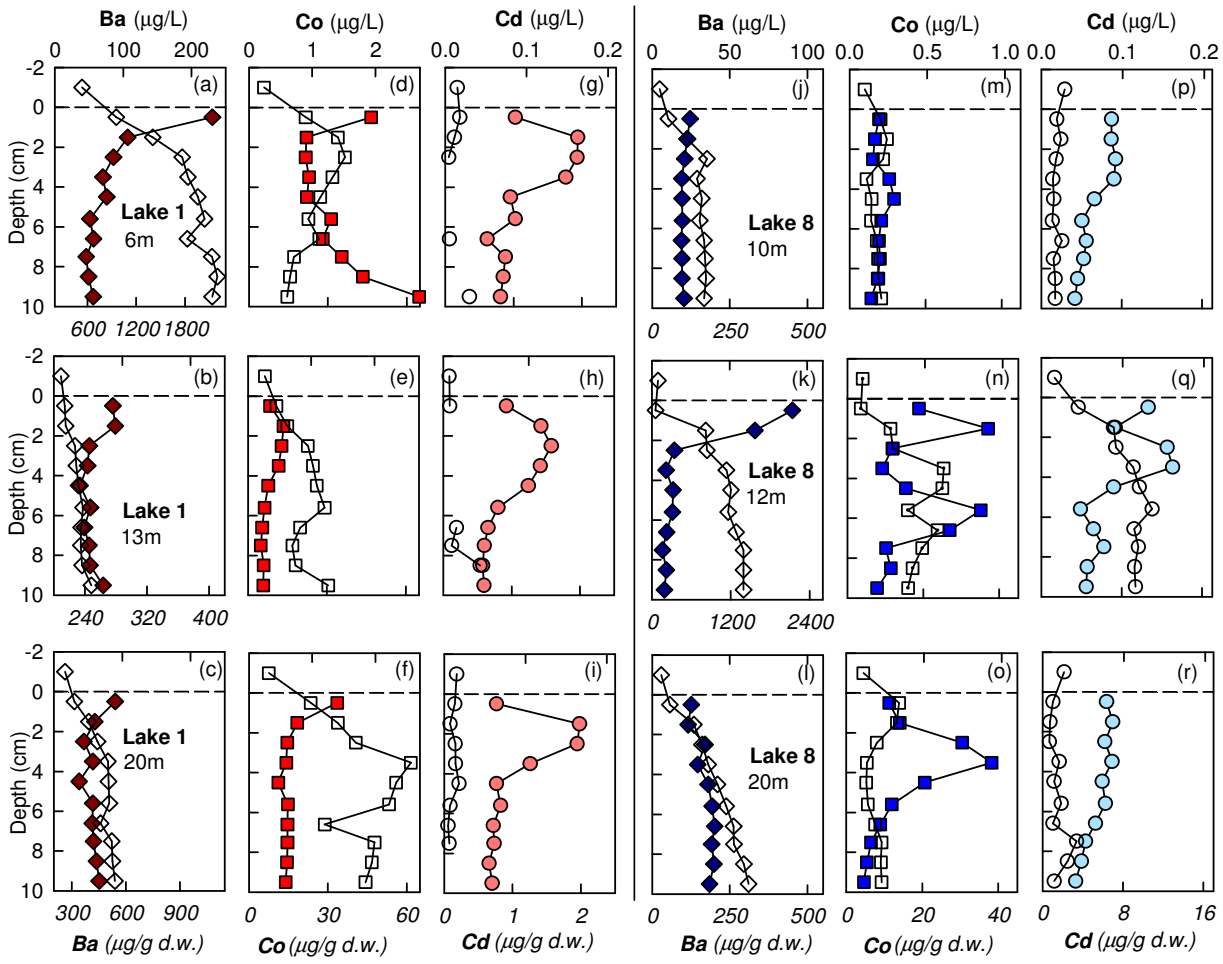

489

490 **Figure 4.** Depth profiles of sedimentary (closed symbol) and porewater (open symbol) Ba (a-c, j-

491 l), Co (d-f, m-o), and Cd (g-i, p-r) in Lake 1 (left panels a-i) and Lake 8 (right panels j-r).

492 Horizontal dashed lines indicate the sediment-water interface.

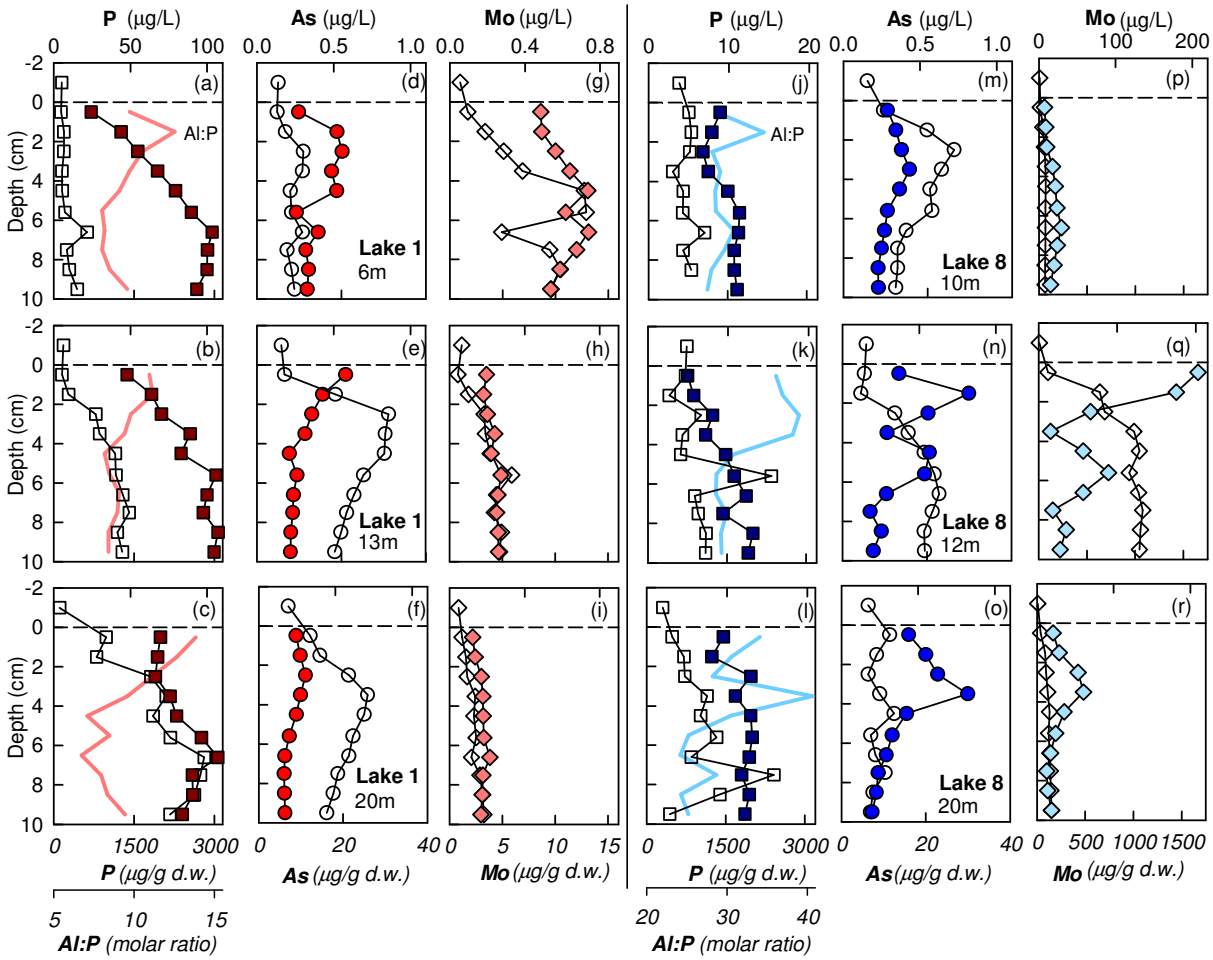

493

494 **Figure 5.** Depth profiles of sedimentary (closed symbol) and porewater (open symbol) P (a-c, j-
495 l), As (d-f, m-o), and Mo (g-i, p-r) in Lake 1 (left panels a-i) and Lake 8 (right panels j-r). Thick
496 solid lines indicate Al:P molar ratios in Lake 1 (a-c) and Lake 8 (j-l). Horizontal dashed lines
497 indicate the sediment-water interface.